Evaluation of the Electrostatic Effect of the 5′-Phosphate of the Flavin Mononucleotide Cofactor on the Oxidation−Reduction Potentials of the Flavodoxin from *Desulfovibrio vulgaris* (Hildenborough)†

Zhimin Zhou‡ and Richard P. Swenson*

Department of Biochemistry, The Ohio State University, Columbus, Ohio 43210

Received May 7, 1996; Revised Manuscript Received July 18, 1996⊗

ABSTRACT: Two mutants of the *Desulfovibrio vulgaris* flavodoxin, T12H and N14H, were generated which, for the first time, place a basic residue within the normally neutral 5′-phosphate binding loop of the flavin mononucleotide cofactor binding site found in all flavodoxins. These histidine residues were designed to form an ion pair with the dianionic 5′-phosphate, either altering its ionization state or offsetting its negative charge to allow evaluation of the magnitude of its electrostatic effect on the redox properties of the cofactor. The midpoint potential for the oxidized/semiquinone couple was not significantly altered in either mutant. However, the midpoint potentials for the semiquinone/hydroquinone couple ($E_{sq/hq}$) were less negative than that of the wild type, increasing by 28 and 15 mV relative to that of the wild type for the T12H and N14H mutants, respectively, at pH 6. ^{31}P NMR spectroscopy suggests that, just as for wild type, the phosphate group in each mutant does not change its ionization state between pH 6 and 8. Therefore, the small increases in midpoint potential must be linked to the protonation of the histidine residues, either through favorable interactions with the anionic hydroquinone or by the partial compensation of the charge on the 5′-phosphate. Values for the pK_a of His12 and His14 in the oxidized flavodoxin were determined by ^{1}H NMR spectroscopy to be 6.71 and 6.93, respectively, which are only modestly elevated relative to the average value for histidines in proteins. This suggests that the histidines do not form strong ion-pairing interactions with the phosphate and/or that the *effective* charge on the 5′-phosphate may be substantially less than the reported formal dianionic charge. Either way, the data provide evidence for the rather weak electrostatic interaction between a charged group at this site and the anionic flavin hydroquinone. In contrast, $E_{sq/hq}$ reported for the apoflavodoxin−riboflavin complex, which lacks the 5′-phosphate group, is 180 mV less negative than that of the native flavodoxin. The re-evaluation of the redox and cofactor binding properties of the riboflavin complex generated values for the dissociation constants for the riboflavin complex in the oxidized, semiquinone, and hydroquinone oxidation states that are 2100-, 63000-, and 54-fold higher, respectively, than that for the naturally occurring flavin mononucleotide complex. The large redox potential shifts observed for both redox couples in the riboflavin complex are primarily the consequence of a decreased stabilization of the semiquinone rather than the result of the absence of the negative charge of the 5′-phosphate. It is concluded from this study that the negative charge on the phosphate group of the cofactor does not play a disproportionate role in decreasing $E_{sq/hq}$, at most contributing equivalently with the acidic amino acid residues clustered around the flavin to an unfavorable electrostatic environment for the formation of the flavin hydroquinone anion.

Flavodoxins are small acidic proteins that contain 1 equiv of flavin mononucleotide (FMN[1]) as their only redox center and function as low-potential, one-electron carriers [for a recent review, see Mayhew and Tollin (1992)]. A distinguishing feature of the flavodoxin family is the very negative reduction potential for the semiquinone/hydroquinone (sq/hq) couple of the bound FMN cofactor (usually <-400 *versus* -172 mV of free FMN, Draper & Ingraham, 1968), placing the flavodoxin among those flavoproteins with the lowest reduction potentials. Flavodoxins share at least three prominent structural characteristics of the FMN binding site that could contribute to this shift, including a largely apolar environment provided by at least one aromatic flanking residue, an asymmetric distribution of charged amino acid residues characterized by a clustering of acidic residues around the cofactor binding site, and an unusual neutral binding site for the 5′-phosphate group of the FMN (Mayhew & Ludwig, 1975; Ludwig & Luschinsky, 1992). Recent studies from our laboratory have directly demonstrated that the apolar flavin environment provided by the tyrosine residue shielding the *si* face of the isoalloxazine ring from solvent and the negative electrostatic environment provided by the clustered acidic residues contribute 51 and 34%, respectively, of the total redox potential shift for the sq/hq couple for the wild-type flavodoxin from *Desulfovibrio vulgaris* as compared to that of the unbound cofactor (Swenson & Krey, 1994; Zhou & Swenson, 1995).

† This study was supported by Grant GM36490 from the National Institutes of Health.

* To whom correspondence should be addressed: Department of Biochemistry, 776 Biological Sciences Bldg., The Ohio State University, 484 W. 12th Ave., Columbus, OH 43210-1292. Telephone: 614-292-9428. Fax: 614-292-6773.

‡ Present address: Department of Biochemistry, Duke University Medical Center, Durham, NC 27710.

⊗ Abstract published in *Advance ACS Abstracts,* September 1, 1996.

[1] Abbreviations: FMN, flavin mononucleotide; EDTA, ethylenediaminetetraacetic acid; $E_{ox/sq}$, midpoint potential for the oxidized/semiquinone couple; $E_{sq/hq}$, midpoint potential for the semiquinone/hydroquinone couple.

S0006-2960(96)01086-0 CCC: $12.00

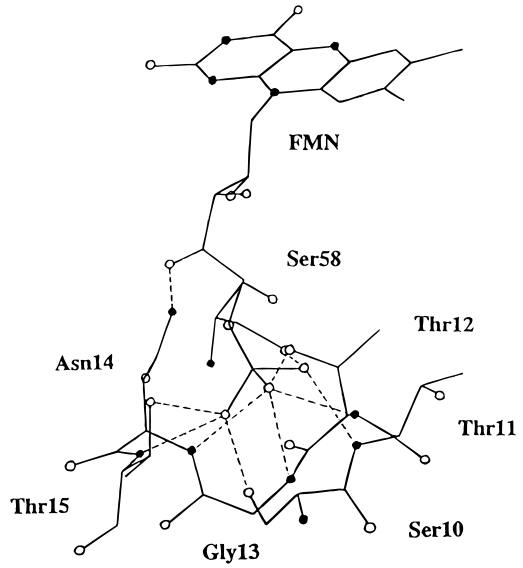

FIGURE 1: Representation of the hydrogen-bonding network in the phosphate binding site. Oxygen atoms are represented as open circles and nitrogen atoms as filled circles. Hydrogen-bonding interactions are indicated by dashed lines. The structure is derived from the X-ray crystal coordinates of Watt *et al.* (1991).

Because electrostatic interactions appear to play an important role in the regulation of the reduction potential of the sq/hq couple, the effect of other charged groups near the cofactor requires evaluation. One such group is the 5′-phosphate moiety of the FMN cofactor itself, which has been reported to be in its dianionic form above pH 6.0 in the flavodoxins from *Megasphaera elsdenii*, *D. vulgaris*, and *Clostridium beijerinckii* (Moonen & Müller, 1982; Vervoort *et al.*, 1986a). The phosphate group is bound in an unusual and highly conserved binding site within the flavodoxin protein (Mayhew & Ludwig, 1975). Interactions occur through an extensive hydrogen-bonding network made up of amide groups in the peptide backbone and neutral amino acid side chains, many of which are provided by hydroxyamino acids (Figure 1) (Watt *et al.*, 1991; Peelen & Vervoort, 1994). These interactions seem to contribute significantly to the tight binding of the cofactor (the K_d for the oxidized FMN is in the subnanomolar range) because riboflavin, lacking the phosphate group, binds much more weakly to most flavodoxin proteins (Curley *et al.*, 1991; Mayhew & Tollin, 1992). The notable absence of basic residues within this phosphate binding site precludes the compensation of the negative charges on the phosphate through direct ion-pairing interactions (Watt *et al.*, 1991). This has led to speculation that the dianionic phosphate group, located only 9−10 Å from the FMN N1 atom, could contribute to the low reduction potentials for the sq/hq couple through unfavorable electrostatic interactions between the phosphate and the negative charge that develops on the hydroquinone as the cofactor becomes fully reduced (Moonen *et al.*, 1984). Several studies seem to support this concept. A recent study in our laboratory directly demonstrated that the electrostatic field provided by negatively charged acidic amino acid residues clustered around the cofactor binding site substantially lowers the midpoint potential of the sq/hq couple ($E_{sq/hq}$) in the flavodoxin from *D. vulgaris* (Zhou & Swenson, 1995). When the apoflavodoxin from *M. elsdenii* is reconstituted with riboflavin 3′,5′-bisphosphate, $E_{sq/hq}$ is shifted from −390 to −410 mV at pH 7.05. This rather modest change was attributed to the additional unfavorable electrostatic interaction between the partially ionized 3′-phosphate group and the anionic flavin hydroquinone (Vervoort *et al.*, 1986b). In contrast, the midpoint potential for the sq/hq couple of the riboflavin complex of the *D. vulgaris* apoflavodoxin is substantially less negative than that for the FMN complex (−262 mV at pH 6.50) (Curley *et al.*, 1991). Can this large change in midpoint potential be directly attributed to the absence of the electrostatic effects of the 5′-phosphate, or is it the result of differences in the binding of this flavin derivative? Theoretical calculations have raised the possibility that the monopole−monopole interaction between the phosphate and the hydroquinone anion could shift $E_{sq/hq}$ by as much as −180 mV (Moonen *et al.*, 1984). However, Ludwig *et al.* (1990) have proposed that electrostatic interaction between a negatively charged group in the protein is more important than the phosphate group in terms of electrostatic interaction in determining redox potentials. Our own work involving the neutralization of surface acidic residues suggests that the electrostatic effects of the phosphate dianion should be modest (Zhou & Swenson, 1995). However, due to the uncertainty in the contribution of the phosphate group in establishing the reduction potential of the flavin, more direct experimental evidence is required.

In this study, the electrostatic effect of the 5′-phosphate group on the FMN cofactor on the redox potentials of the flavodoxin was evaluated by introducing a basic histidine residue at two different positions in the phosphate binding loop in the flavodoxin from *D. vulgaris*. Two histidine mutant flavodoxins, T12H and N14H, were generated, purified, and characterized. The ionization properties and possible charge−charge interaction between the phosphate group and the imidazole side chain were studied by both ^{31}P and ^{1}H NMR. The electrostatic contribution of the phosphate group to the negative redox potential of the wild-type flavodoxin is evaluated and discussed.

EXPERIMENTAL PROCEDURES

Materials. Anthraquinone-2,6-disulfonate, 2-hydroxy-1,4-naphthoquinone, and safranine T were purchased from Fluka Chemicals. Safranine T was recrystallized before use. Benzyl and methyl viologen were obtained from Serva Chemicals. β-Hydroxyethyl viologen was synthesized as described previously (Kazarinova *et al.*, 1967; Zhou & Swenson, 1995). Riboflavin was obtained from Eastman Kodak. The Sequenase Version 2.0 DNA sequencing kit was obtained from United States Biochemical Corp. The Muta-Gene *in vitro* mutagenesis kit was from Bio-Rad Laboratories. The restriction enzymes *Hin*dIII, *Nco*I, and *Nci*I were obtained from GIBCO BRL. Deuterium oxide-d_2 (D_2O) was from Norell, Inc. Deuterium chloride (DCl), sodium deuteroxide (NaOD), and sodium 3-(trimethylsilyl)-propionate-2,2,3,3-d_4 were obtained from Cambridge Isotope Laboratories. All other chemicals were of analytical reagent grade.

Bacterial Strain and Plasmids. The pseudo wild-type flavodoxin gene (P2A) from *D. vulgaris* (Hildenborough) (NCIB 8303/ATCC 29579) has been previously cloned into the *p*BUC*tac* expression vector and characterized (Krey *et al.*, 1988). The pseudo wild-type flavodoxin produced from this construction, which differs from the wild-type protein in that an alanine residue replaces proline at position 2 for increased efficiency of expression in *Escherichia coli*, has properties identical to those of the wild-type protein in every

way tested. In this study, the P2A gene was subcloned into the *p*Bluescript KS plasmid (Strategene) for oligonucleotide-directed mutagenesis and overexpression (Zhou & Swenson, 1995).

Molecular Modeling. Mutant proteins, in which a histidine residue replaces one of the amino acid residues in the phosphate binding loop, were designed and evaluated within the context of retaining hydrogen-bonding interactions between the imidazole group and the cofactor (primarily with the 5′-phosphate) similar to those in the wild-type protein. Direct interactions could either alter the pK_a and ionization state of the phosphate or form strong ion-pairing interactions. The amino acid residues targeted for substitution were selected with the assistance of the geometry optimization of the mutant structure using the AMBER molecular mechanical force field (Weiner *et al.*, 1986) within the HyperChem molecular-modeling software (Autodesk, Inc.). After a particular amino acid had been substituted with histidine, all amino acid residues within an 8 Å radius sphere centered at the β-carbon of the substituted residue were selected for energy minimization. Partial charges on the atoms of the FMN phosphate group were assigned on the basis of the AMBER parameters for the nucleotide monophosphate (net charge of -1.6), and the substituted histidine side chain was given net charge of $+1$ by selecting the "Hip" template. A distance-dependent dielectric parameter and switched cutoff in the range of 8−15 Å were selected for force field options. The calculation proceeded using the Polak−Ribiere conjugate gradient algorithm and was terminated when the RMS gradient reached a value of 0.1 kcal Å^{-1} mol^{-1}. Structures with various manually adjusted torsion angles for the histidine side chain were also geometry optimized to explore alternative ion-pairing or hydrogen-bonding interactions with the phosphate group and to evaluate each local *versus* global energy minimum.

Side-Directed Mutagenesis. Oligonucleotide-directed mutagenesis was carried out using the Kunkel (1985) method for selection biased toward the mutant constructions. Two degenerate oligonucleotides were used: 5′-CCGTGTTGCCATGGGTGGAACCG-3′ for T12H and 5′-CGGTGTATTCCGTGTG(C)CC(G)GTGGTGGAACCG-3′ for N14H. The underlined nucleotides are different from those of the wild type, and those in parentheses are "silent" mutations introduced to assist in screening by differential restriction mapping. For the T12H mutation, a new *Nco*I site was created. A new *Nci*I site was introduced by the N14H mutation. All the mutations as well as the sequence integrity of the entire structural gene were confirmed by the Sanger dideoxy termination DNA sequencing procedure using the Sequenase protocol (Sanger *et al.*, 1977).

Purification of Expressed Mutant Flavodoxin Proteins. Transformed *E. coli* AG-1 cells were cultured for up to 48 h at 37 °C in NZY medium containing 100 μg/mL ampicillin. Flavodoxin was purified by procedures described previously (Zhou & Swenson, 1995) except that the NaCl concentrations of the wash and elution solutions used during ion exchange chromatography were adjusted to accommodate the change in the net charge of the mutants. The A_{274}:A_{458} absorbance ratios of the purified mutant flavodoxin preparations were *ca.* 4.0, and the proteins were judged to be homogeneous by SDS−polyacrylamide gel electrophoresis.

Redox Potential Measurements. Midpoint potentials were determined by equilibration with redox indicator dyes using procedures described previously (Zhou & Swenson, 1995). In the evaluation of the pH dependencies of the reduction potentials, the E_m values for anthraquinone-2,6-disulfonate ($E_{m,7} = -184$ mV; Dutton & Baltscheffsky, 1972) and safranine T ($E_{m,7} = -276$ mV; Clark, 1972) were calculated according to the pH dependencies reported by Clark (1972). Because the midpoint potentials of benzyl viologen and β-hydroxyethyl viologen are pH-independent throughout the pH range of this study (Bird & Kuhn, 1981), the $E_{m,7}$ values were used to establish the reduction potentials of the sq/hq couple.

^{31}P and ^{1}H NMR Spectroscopy. All NMR samples contained 2.0 mM flavodoxin. Samples for ^{31}P NMR measurements were prepared in 50 mM Tris·HCl buffer (pH 6−8). The final sample volume was *ca.* 3 mL and contained 10% (v/v) D_2O to aid in locking the magnetic field. The ^{31}P NMR spectra were recorded using 10 mm NMR tubes at 300 K on a Bruker MSL-300 NMR spectrometer operating at 60.8 MHz. ^{31}P chemical shifts were determined relative to an external standard of 85% phosphoric acid. Flavodoxin samples for ^{1}H NMR spectroscopy were prepared in 20 mM sodium phosphate buffer (pH 7) and exchanged into D_2O by repeated lyophilization followed by solvation in 99.8% D_2O. The ^{1}H NMR spectra were recorded at 300 K on a Bruker AM-500 NMR spectrometer. Proton chemical shifts were determined relative to an internal standard of 70 μM sodium 3-(trimethylsilyl)propionate-2,2,3,3-d_4 which was assigned a chemical shift value of 0.0 ppm. In both measurements, the pH of the sample solutions was adjusted by adding appropriate volumes of 5% (v/v) NaOD or DCl in D_2O. The reported pH values (pH*) are not corrected for the deuterium effect. Data were processed on an Indigo workstation (Silicon Graphics, Inc., Mountain View, CA) using Felix 2.30 software from Biosym Technologies, San Diego, CA.

Preparation of the Wild-Type Apoflavodoxin−Riboflavin Complex. Apoflavodoxin was prepared as described previously (Wassink & Mayhew, 1975). Briefly, the flavodoxin solution was mixed with an equal volume of 10% (w/v) cold trichloroacetic acid in 0.10 M potassium phosphate buffer (pH 7.0) containing 0.30 mM ethylenediaminetetraacetic acid (EDTA) at 4 °C in darkness for 10 min. The mixture was centrifuged for 10 min in an Eppendorf microfuge, and the yellow supernatant was discarded. The whitish protein precipitate was washed with 5% trichloroacetic acid in 0.10 M potassium phosphate buffer (pH 7.0) containing 0.30 mM EDTA, and the mixture was centrifuged as before. After three washes, the pellet was dissolved in 1.5 mL of 0.10 M potassium phosphate buffer (pH 7.0) containing 0.30 mM EDTA and dialyzed against the same buffer at 4 °C. Apoflavodoxin was stored at 4 °C and was never frozen. The riboflavin−apoflavodoxin complex was prepared by mixing riboflavin and apoflavodoxin solutions in darkness at room temperature. The mixture was passed through a Sephadex G-50 column (2.5 × 50 cm) to remove the excess riboflavin.

Determinations of Apoflavodoxin and Riboflavin Concentration. On the basis of the amino acid composition and the extinction coefficients for tryptophan (5698 M^{-1} cm^{-1}) and tyrosine (1280 M^{-1} cm^{-1}) (Elwell & Schellman, 1977), the molar extinction coefficient at 280 nm of unfolded *D. vulgaris* apoflavodoxin was calculated to be 17 780 M^{-1} cm^{-1}. An apoflavodoxin sample was determined by its absorbance at 280 nm after denaturation in 6 M guanidine hydrochloride in 10 mM phosphate buffer (pH 7.0). The

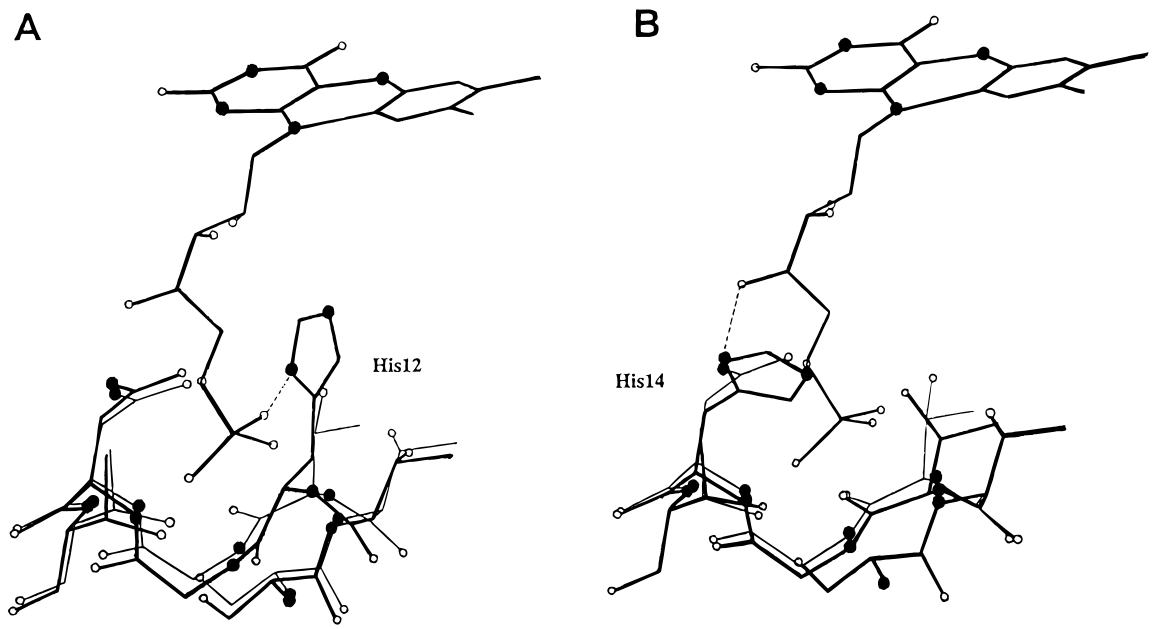

FIGURE 2: Comparison of the structure of the binding site for the 5′-phosphate of the FMN of the histidine mutants (thick line) to that of the wild-type flavodoxin (thin line) from *D. vulgaris*. Oxygen atoms are represented as open circles and nitrogen atoms as filled circles. Possible hydrogen bonds between the mutated histidine residue and the FMN cofactor are indicated by dashed lines. The wild-type structure is based on the X-ray crystal data of Watt *et al.* (1991), while those of the mutants are based on geometry-optimized modeled structures (see Experimental Procedures): (A) T12H *versus* the wild type and (B) N14H *versus* the wild type.

riboflavin concentration was determined by its absorbance at 445 nm using a molar extinction coefficient of 12 500 M^{-1} cm^{-1}.

Determination of the Dissociation Constants for the Oxidized and Fully Reduced Riboflavin Complex. The K_d value for the binding of riboflavin to apoflavodoxin was determined by difference spectrophotometric titration. A 25 μM solution of riboflavin in 50 mM sodium phosphate buffer (pH 7.0) was titrated by the addition of a substoichiometric amount of a 500 μM stock solution of purified apoflavodoxin in the same buffer. After equilibrium was reached, the visible absorption spectrum was recorded on a Hewlett-Packard Model 8452A diode array spectrophotometer at 25 °C and corrected for dilution. The titration continued until no further absorbance changes were observed. Difference spectra were generated by subtracting the starting riboflavin spectrum from each spectrum recorded during the titration. The fraction of bound riboflavin was calculated from the absorbance changes at 496 and 440 nm in the difference spectrum. The K_d was determined by averaging eight points near the equivalence point of a plot of the fraction of riboflavin bound *versus* the total apoflavodoxin concentration.

The K_d value for the reduced riboflavin complex was determined using the following fluorescence method. It is commonly assumed that all species of reduced alloxazines and isoalloxazines, both free and protein-bound, are nonfluorescent under the usual experimental conditions (Ghisla *et al.*, 1974). The protein fluorescence of the *D. vulgaris* flavodoxin holoprotein is effectively quenched, and its emission spectrum could not be measured (D'Anna & Tollin, 1972; Dubourdieu *et al.*, 1975). Therefore, the concentration of the apoflavodoxin in equilibrium with the reduced riboflavin−apoflavodoxin complex could be determined according to its protein fluorescence. A solution of apoflavodoxin and riboflavin in 50 mM phosphate buffer (pH 7.0) containing 0.30 mM EDTA was reduced by light irradiation anaerobically. The fluorescence emission at 350 nm of the apoflavodoxin excited at 290 nm was recorded at ambient temperature on a SLM Aminco SPF-500C spectrofluorimeter. The concentration of the apoflavodoxin remaining at equilibrium was calculated on the basis of the linear correlation between the protein fluorescence and the apoflavodoxin concentration obtained using the same apoprotein preparation, on the same day, and under the same experimental conditions. The dissociation constant of the reduced riboflavin complex was determined by the average of two different measurements with riboflavin concentrations of 32 and 100 μM, respectively.

RESULTS

Generation, Expression, and Characterization of the Histidine Mutants. The X-ray crystal structure (Watt *et al.*, 1991) and NMR studies (Peelen & Vervoort, 1994) of the *D. vulgaris* flavodoxin suggest that Thr12 and Asn14 are among several amino acid residues that form an extensive hydrogen-bonding network with the phosphate group. Interactions involve the peptide backbone NH group of both residues as well as the β-hydroxyl group of Thr12. The amide group of the Asn14 side chain may also hydrogen bond to the 4′-hydroxyl group of the ribityl side chain of the cofactor. Molecular-modeling studies suggested that flavodoxins containing the T12H or N14H substitutions can form a phosphate binding loop similar to that of the wild type. The imidazole side chain in these mutants can form hydrogen-bonding interactions with the cofactor similar to those with the wild-type residues (Figure 2A,B). Consequently, these substitutions should minimally affect the binding energy with cofactor, reducing such indirect effects on the redox potential. However, for the first time in a flavodoxin, these mutations place a basic residue immediately adjacent to the phosphate group, changing the electrostatic characteristics of this binding site and possibly allowing for direct ion pairing and charge compensation and/or altering the ionization state of the phosphate itself. Because of the ionization properties of the histidine side chain, the intensity

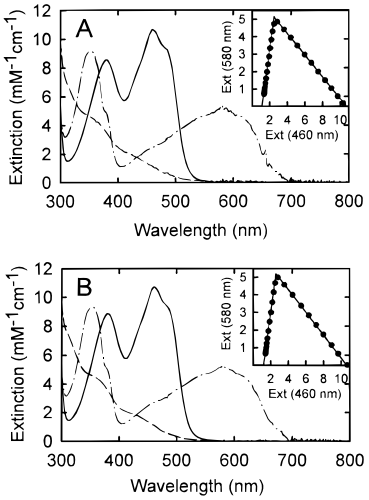

FIGURE 3: Ultraviolet−visible absorbance spectra of the T12H mutant (A) and the N14H mutant (B) flavodoxins during reduction with sodium dithionite under anaerobic conditions. Flavodoxin (*ca.* 30 μM) in 50 mM sodium phosphate buffer (pH 7.0) was titrated under argon in a sealed titration cuvette at 25 °C: solid line, oxidized; dot-dashed line, semiquinone; and dashed line, fully reduced. In each case, the spectrum of the fully formed semiquinone was generated by the subtraction of the contribution of the small amount of oxidized species present near the midpoint of the titration and rescaled to 100%. Similarly, the hydroquinone spectrum was corrected for the presence of a small amount of semiquinone remaining at the end of the titration. The insets show absorbance changes at 580 nm *versus* those at 460 nm during the course of the titration showing the separation of each couple (extinction values in units of mM^{-1} cm^{-1}).

of the electrostatic interaction between the isoalloxazine ring and the phosphate group can be evaluated as a function of the charge on the histidine.

The T12H and N14H mutant flavodoxins were generated using standard oligonucleotide-directed mutagenesis technology (Kunkel, 1985). Each mutant protein was overexpressed in *E. coli* AG-1 cells as the holoprotein, accumulating in the cells in the partially reduced or semiquinone state as indicated by the dark bluish color of the bacterial pellet. This is similar to what is observed for the wild type and other mutant flavodoxins (Krey *et al.*, 1988; Swenson & Krey, 1994; Zhou & Swenson, 1995). The fully oxidized purified holoproteins in each case had A_{274}:A_{458} ratios of 4.1 ± 0.1, which is similar to that for the wild type and is consistent with a 1:1 stoichiometry for FMN binding, indicating that cofactor binding was not grossly affected by the mutations.

The visible absorbance spectra of all three oxidation states were determined for both mutant flavodoxins during titration with sodium dithionite. As shown in Figure 3 (panel A, T12H; and panel B, N14H), the spectra were essentially identical to those of the wild-type flavodoxin (Swenson & Krey, 1994). In both cases, the semiquinone state was seen to accumulate to nearly stoichiometric levels during the titration (see insets), suggesting that the reduction potentials of the two redox couples remain well-separated as in the wild-type protein. These observations also imply that the structural alternations introduced by each mutation were limited locally to the phosphate binding site, which should make data interpretation less complex.

The midpoint potential of the ox/sq couple ($E_{ox/sq}$) for both mutants was determined by equilibration with the redox indicator dye anthraquinone-2,6-disulfonate ($E_{m,7}$ = −184 mV, Dutton & Baltscheffsky, 1972). Values for $E_{ox/sq}$ of −189 mV for the T12H mutant and −188 mV for the N14H mutant were obtained at pH 7.0. These values are very similar to that determined for the recombinant wild-type flavodoxin using this indicator dye under these conditions ($E_{ox/sq}$ = −185 ± 4 mV). Also, midpoint potentials for this couple for the two mutants as determined using 2-hydroxy-1,4-naphthoquinone ($E_{m,7}$ = −145 mV, Cammack *et al.*, 1977) as the indicator dye are similar to reported values for the wild type (Swenson & Krey, 1994). It can be concluded, therefore, that the histidine substitutions have little effect on the reduction potentials of the ox/sq couple.

The midpoint potential of the sq/hq couple was also determined for both mutants by equilibration with the indicator dye β-hydroxyethyl viologen ($E_{m,7}$ = −408 mV, Homer *et al.*, 1960). Values for $E_{sq/hq}$ of −422 mV for T12H and −426 mV for N14H were obtained at pH 7.0. Thus, both histidine substitutions have increased the midpoint potential of this couple compared to that of the wild type having an $E_{sq/hq}$ value of −443 mV under similar conditions. However, these increases are relatively small, being 21 mV for the T12H mutant and 17 mV for the N14H mutant. The original design of these mutants proposes favorable ion-pairing interactions between the protonated histidine and the dianionic 5′-phosphate group leading to charge compensation and/or the alteration of the pK_a of the phosphate itself. At pH 7.0, the histidine residues may only be partially protonated so the full effects may not be elicited. It is also not possible to determine whether the changes in the reduction potentials are the consequence of the ionization state of the histidines or the phosphate group. The following experiments were designed to test these possibilities.

Redox-Linked pH Dependency of the T12H, N14H, and Wild-Type Flavodoxins. The midpoint potentials for the ox/sq couple of the T12H and N14H mutants displayed a pH dependency of −65 and −66 mV per pH unit, respectively. These values are similar to that of wild type and conform reasonably well to the theoretical value of −59 mV for a single-proton transfer linked to the one-electron reduction of the flavin, maintaining the neutral semiquinone throughout this pH range as observed. If ionization of the mutated histidine occurs in this pH range as expected (see also the following ^{1}H NMR experiments), this general pH dependency implies that there is little or no preferential interaction of either the neutral or the protonated forms of the histidine with the neutral flavin semiquinone in the mutant flavodoxin.

The pH dependency of $E_{sq/hq}$ over the range of 5.5−8.3 was established for the wild-type flavodoxin and two histidine mutants. Just as observed previously for this and other flavodoxins, the midpoint potential of the wild-type flavodoxin increased at pH values below 7.0 (Ludwig & Luschinsky, 1992). However, the $E_{sq/hq}$ values of both the T12H and N14H mutants were generally less negative than that of the wild type at all pH values tested, with the difference becoming more pronounced at lower pH values (Figure 4). It should be emphasized that these data represent the difference between two experimental values, *i.e.* the midpoint potentials of the mutants and the wild type determined under identical conditions, resulting in some scatter. At pH values around 8.0, the $E_{sq/hq}$ value of N14H was very close to that of the wild type, but a 10 mV difference between the values for T12H and the wild-type flavodoxin seems to remain. This 10 mV difference may not result from the ionization of His12. Instead, it could be due to small alternation in the hydrogen-bonding network (see below). The pH dependency of both mutants could be

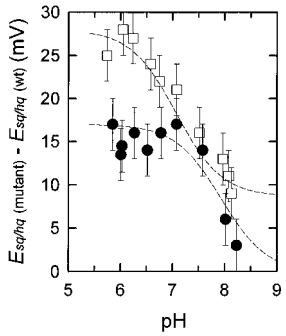

FIGURE 4: pH dependency of the midpoint potentials for the sq/hq couple of the T12H mutant (open squares) and N14H mutant (filled circles) flavodoxins at 25 °C relative to that of the wild type. At each pH value, the difference between the midpoint potential of the mutant and that for the wild-type flavodoxin is plotted. The dashed lines represent a fit of the data to a redox-linked ionization model as described in Swenson and Krey (1994) (see Results for details).

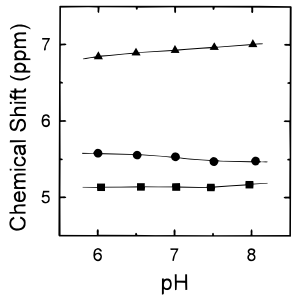

FIGURE 5: pH dependency of the ^{31}P NMR signal for the 5′-phosphate of the FMN cofactor bound to the T12H mutant (triangles), N14H mutant (circles), and the wild-type (square) flavodoxins at 27 °C. Chemical shift values are relative to an external standard of 85% phosphoric acid.

fit to a redox-linked ionization mechanism in which the reduction potential of the FMN is coupled to the protonation of an ionizable group in each mutant protein [see Swenson and Krey (1994)]. In each mutant, the shift in the midpoint potential upon protonation is approximately 15−18 mV which is coupled to a modest shift in the pK_a of the ionizable group of 0.1−0.2 unit upon reduction of the flavin. On the basis of the curve fitting to this model, the pK_a values of the ionizable group in the T12H and N14H mutants linked to the midpoint potential shifts were 7.0 ± 0.3 and 7.8 ± 0.4, respectively. Given these pK_a values, it is possible that the pH dependency of the midpoint potentials could result from ionization of either the phosphate group or the substituted histidine residue. The ionization properties of the 5′-phosphate and the introduced histidine residue for each mutant in its fully oxidized state were characterized as follows.

^{31}P NMR Experiments of the T12H, N14H, and Wild-Type Flavodoxins. It has been reported that the 5′-phosphate group remains in its dianionic form above pH 6.0 in the oxidized flavodoxins from *M. elsdenii*, *D. vulgaris*, and *C. beijerinckii* flavodoxins (Moonen & Müller, 1982; Vervoort *et al.*, 1986a). In this study, the ionization state of the phosphate group in the T12H, N14H, and wild-type flavodoxins was monitored over the pH range of 6.0−8.0 by ^{31}P NMR spectroscopy (Figure 5). The 5′-phosphate resonance in the wild-type flavodoxin was observed at a low-field position of 5.1 ppm and remained unchanged throughout this pH range, consistent with the published reports. The phosphate resonance in each mutant also appeared at low field, remaining relatively constant throughout the pH range of 6−8. At each pH value, the chemical shift value for each mutant was shifted downfield relative to that of the wild-type protein, about 0.4 ppm in the N14H and 1.8 ppm in the T12H mutant. Because ^{31}P chemical shifts of phosphate esters are sensitive to the strength and angle of phosphate−oxygen bonds (Gorenstein, 1981), the small downfield shift of the resonance peak in the N14H mutant suggests that the geometry and/or environment of phosphate might only be slightly altered in this mutant. In contrast, the larger downfield shift of the resonance in the T12H mutant may reflect the loss of the hydrogen bond between the phosphate and the γ-OH of the Thr12 side chain in the T12H mutant.

The chemical shift of the phosphate group in each mutant displayed only a very small pH dependency, far less than reported for a change in ionization state which can be as much as 4 ppm for phosphate monoesters in solution (Gorenstein, 1981). Small differences in the chemical shifts were noted, however. Attempts were made to fit these small changes to the ionization of the adjacent histidine in each case. This was not possible for the T12H mutant; however, for the N14H mutant, the data could be fit to a single ionization with an apparent pK_a value of 7.01 ± 0.09. Taken together, the NMR data seem to suggest that the 5′-phosphate group in both the T12H and N14H mutant flavodoxins remains in its dianionic form, perhaps, being affected slightly by the ionization of the His14 in the N14H mutant and the loss of a hydrogen bond in the T12H mutant; however, the role of geometric constraints in establishing the chemical shift of the phosphate must also be considered in the interpretation of these results (Gorenstein, 1981) (see below). Since the pH dependency of the redox potential for the sq/hq couple in each mutant appears not to be the result of a change in the ionization state of the 5′-phosphate group, the focus was switched to the ionization properties of the newly introduced histidine residues.

Determination of the pK_a of His12 and His14 of the T12H and N14H Mutants. The pK_a value of the histidine side chain introduced in the T12H and N14H mutants was determined by monitoring the changes in chemical shift of the C2 and C4 hydrogens on the imidazole ring by ^{1}H NMR titration throughout the pH* range of 5.4−9 using the method described by Markley (1975). As an example, the results obtained during the titration of the T12H mutant are shown in Figure 6. As is otherwise noted, qualitatively similar results were obtained for the N14H mutant (data not shown). Four sharp and well-separated resonance peaks (a−d) were observed in the aromatic region of the ^{1}H NMR spectrum of each mutant and were assigned to the histidine residues on the basis of their pH dependency and general chemical shift values. Wild-type flavodoxin contains only one histidine residue, His142, and the ^{1}H chemical shifts of both nonexchangeable imidazole hydrogens of this residue have been assigned previously in this laboratory (peaks b and d, unpublished results). The other two peaks (a and c), which are absent in the wild type, were assigned to the C2 and C4 hydrogens of either His12 in the T12H mutant or His14 in the N14H mutant.

The chemical shift of the C2 and C4 hydrogens made smooth transitions downfield as the pH was lowered over the range of pH 5.4−9.2. By nonlinear least-squares analysis, the data were found to adequately conform to a modified version of the Hill equation (Markley, 1973). In all cases, the Hill coefficient was observed to be nearly equal

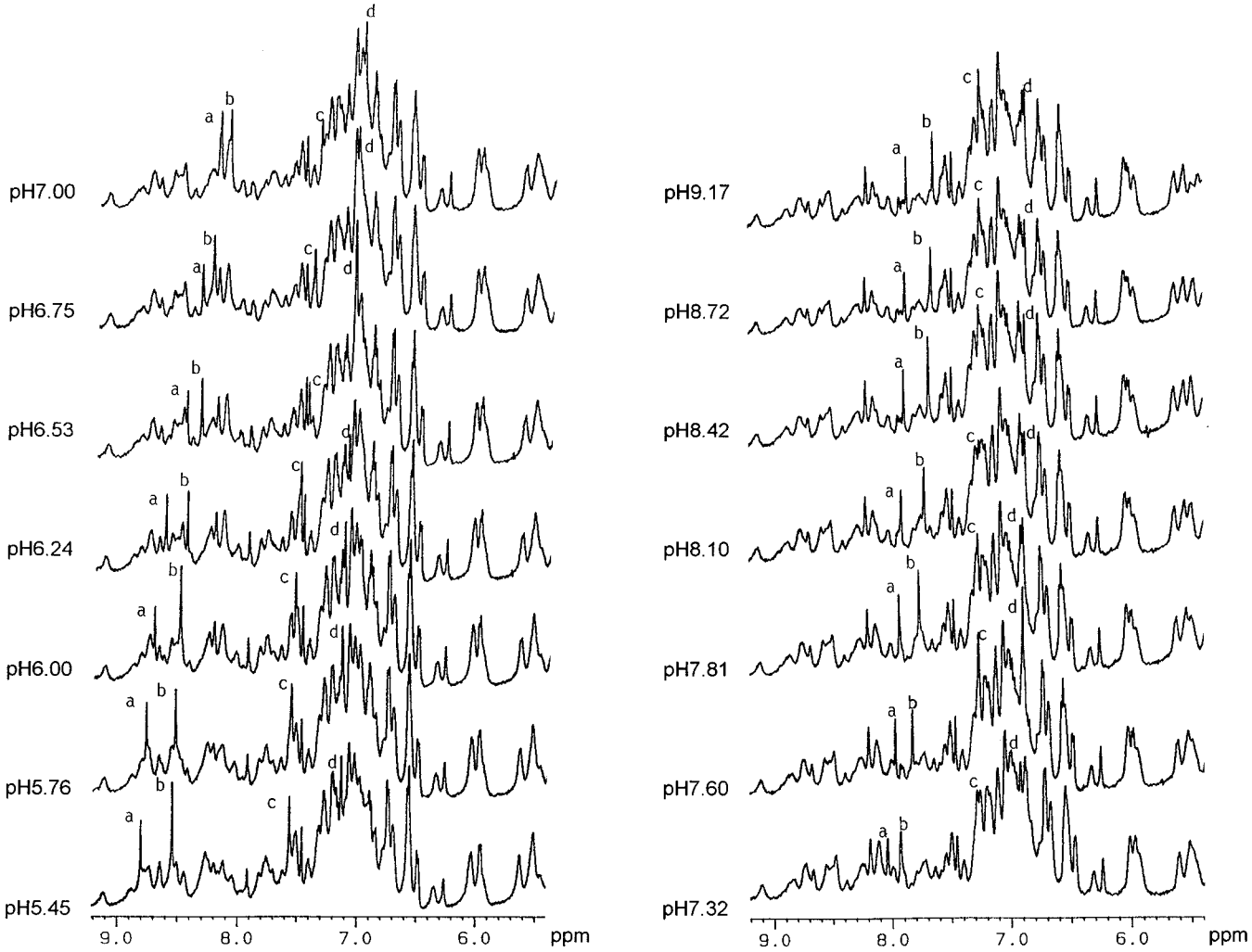

FIGURE 6: 500 MHz ^{1}H NMR spectra in the aromatic region for the T12H mutant flavodoxin as a function of solution pH. Peaks a and c were assigned to the C2 and C4 hydrogens, respectively, of His12; peaks b and d were assigned to the C2 and C4 hydrogens, respectively, of the His142 residue on the basis of analogy to the wild-type spectrum. Chemical shift values are relative to an internal standard of TSP.

to 1. In the T12H mutant flavodoxin, the total chemical shift throughout the pH range was 0.95 ppm for the C2 hydrogen and 0.34 ppm for the C4 hydrogen of the His12 imidazole side chain. The same pK_a value of 6.71 was derived from chemical shifts of each of the two hydrogens (Figure 7A,B). The total chemical shift for His142 was 0.91 ppm for the C2 hydrogen and 0.28 ppm for the C4 hydrogen. The pK_a values obtained for this histidine residue were 7.03 on the basis of the C2 hydrogen signal and 6.93 from the C4 hydrogen (Figure 7A,B), giving an average value of 6.98.

Resonance peaks in similar regions of the ^{1}H spectrum were noted in the N14H mutant flavodoxin; however, both the C2 and C4 resonance peaks for His14 gradually broadened as the pH was increased. The chemical shift for the C4 hydrogen of the His14 was notably broadened even at the lowest pH values attempted. The chemical shifts of both protons could be readily assigned, however, from difference spectra except at pH values greater than 8 where assignments could not be made unambiguously. The pK_a values determined for the C2 and C4 hydrogens of His14 were 6.89 and 6.92, respectively (Figure 7C,D). The pH-dependent resonance peak broadening was determined to be reversible. In a separate ^{1}H NMR titration of the N14H mutant, the pH was adjusted from high (9.24) to low (5.44) values. In this case, the peaks sharpened and similar pK_a values of 6.95 and 6.94 were obtained from the C2 and C4 hydrogen resonances (Figure 7E,F). An average pK_a value for His142 in this mutant was 6.94, similar to those of the wild type and the T12H mutant (Figure 7C,D). The average value of 6.93 for the pK_a of His14 in the N14H mutant is *ca.* 0.2 pH unit higher than that of His12 in the T12H mutant. This value is also in good agreement with the pK_a value of 7.01 ± 0.09 obtained from the small change in the phosphate resonance noted for the N14H mutant during the ^{31}P NMR titration. Both observations may indicate that there is at least a general electrostatic interaction between the phosphate group and the His14 side chain.

The resonance peak broadening could be the result of the immobilization of the neutral form of the His14 side chain during the titration. On the basis of the molecular modeling of these mutants, the side chain of His14 in the N14H mutant seems to be situated in a pocket composed of two β-turns: -Gly128-Asp129-Pro130-Arg131- and -Thr12-Gly13-His14-. The neutral form of the imidazole ring may preferentially interact with residues within this pocket, consistent with the complete reversibility of the broadening event. In contrast, the His12 side chain appears to remain highly mobile throughout the titration on the basis of the very narrow resonance band.

Redox Properties of the Apoflavodoxin−Riboflavin Complex. Certain apoflavodoxins can be reconstituted with riboflavin instead of FMN (Mayhew & Tollin, 1992). This is true for the *D. vulgaris* flavodoxin as well. The binding of riboflavin is associated with characteristic red shifts and

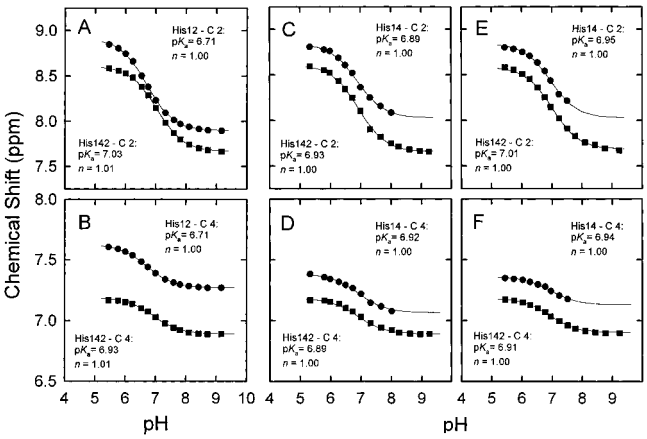

FIGURE 7: ^{1}H NMR titration curves for the histidine C2 and C4 hydrogens of the T12H mutant (A and B) and N14H mutant (C−F) flavodoxins. The pH dependency of the chemical shift assigned to His142 in each protein is represented by the filled squares in each panel. The filled circles depict the chemical shift data for each of the mutants as follows: (A) C2 H of His12, (B) C4 H of His12, (C and E) C2 H of His14 titrated from low to high and from high to low pH, respectively, and (D and F) C4 H of His14 titrated from low to high and from high to low pH, respectively. In each titration, the proton chemical shift data were fit by nonlinear least-squares regression analysis to a modified form of the Hill equation as described by Markley (1975).

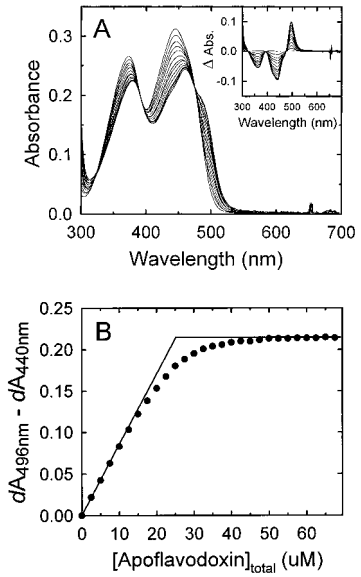

FIGURE 8: Spectral changes associated with the reconstitution of the recombinant *D. vulgaris* apoflavodoxin with riboflavin and the determination of the dissociation constant for the riboflavin complex at pH 7.0. (A) Ultraviolet-visible absorbance spectra of the riboflavin (*ca.* 25 μM) titrated with apoflavodoxin (*ca.* 500 μM in stock solution) at 25 °C. (All spectra were corrected for dilution.) The inset shows difference spectra generated by subtraction of the initial riboflavin spectrum from each spectrum obtained during the titration. (B) Plot of the sum of absorbance changes at 440 and 496 nm obtained from the difference spectra (panel A inset) *versus* the total apoflavodoxin concentration in the titration mixture.

decreased extinction coefficients of the main absorbance peaks of riboflavin as shown in Figure 8A. These absorbance changes are very similar to those observed upon reconstitution of the apoflavodoxin with FMN.

The midpoint potential for the ox/sq couple for the riboflavin complex was determined to be −228 mV by equilibration with the indicator dye anthraquinone-2,6-disulfonate ($E_{m,7}$ = −184 mV) during reduction with dithionite at pH 7.0 (Figure 9A). This value is quite similar to that of riboflavin (−231 mV, Lowe & Clark, 1956) and

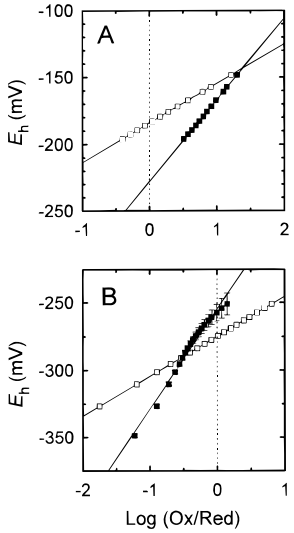

FIGURE 9: Determination of the midpoint potential for the ox/sq couple (A) and sq/hq couple (B) of the riboflavin complex. Reduction potentials were determined during titration with sodium dithionite under strict anaerobic conditions by equilibrium of the riboflavin complex (*ca.* 30 μM) (filled squares) with the following redox indicator dyes: 30 μM anthraquinone-2,6-disulfonate (open squares) in the determination of the ox/sq couple and safranine T (open squares) in the determination of the sq/hq couple. Data were plotted and midpoint potentials established as described in Zhou and Swenson (1995).

FMN (−238 mV, Draper & Ingraham, 1968) in solution but is 80 mV more negative than that of the native flavodoxin−FMN complex (−148 mV, Swenson & Krey, 1994).

The midpoint potential for the sq/hq couple for the riboflavin complex was determined by equilibration with the indicator dye safranine T ($E_{m,7}$ = −276 mV) during reduction with dithionite (Figure 9B). The $E_{sq/hq}$ value was −257 mV, which is 85−90 mV more negative than that of free riboflavin (−167 mV, Draper & Ingraham, 1968) and FMN (−172 mV, Draper & Ingraham, 1968) but is 186 mV less negative than that of the wild-type flavodoxin (−443 mV, Swenson & Krey, 1994). These results are consistent with previously reported midpoint potentials determined at pH 6.50 (Curley *et al.*, 1991).

Determinations of the Dissociation Constants for the Three Oxidation States of the Riboflavin Complex. The dissociation constant (K_d) for the oxidized riboflavin complex was determined from the spectral changes occurring upon titration of riboflavin with apoflavodoxin (Figure 8A) by replotting the changes in absorbance at 496 and 440 nm as a function of added apoprotein (Figure 8B). An average K_d value of 0.51 ± 0.04 μM was determined from eight points near the equivalent point. This value is slightly lower than the previously reported values of 0.77 μM (D'Anna & Tollin, 1972) and 0.72 μM (Curley *et al.*, 1991). However, compared with the K_d value of 0.24 nM reported for the FMN complex of the *D. vulgaris* flavodoxin (Curley *et al.*, 1991), there is at least a 2100-fold decrease in the association of riboflavin to the apoflavodoxin. On the basis of the fact that free energy is path-independent, the dissociation constants for the semiquinone and hydroquinone states of the FMN− and riboflavin−apoflavodoxin complexes can be determined from the shift in midpoint potentials of each couple relative to those of the unbound cofactor according to the free energy relationships defined by the relevant linked equilibria [for example, see Dubourdieu *et al.* (1975)]. The K_d values of 0.45 and 15 μM were calculated for the

Table 1: Properties of the Riboflavin Complex and Comparison with the Wild-Type Flavodoxin

	λ_{max} (nm)		complex dissociation constant			$E_{ox/sq}$	$E_{sq/hq}$
	I	II	K_d (ox)	K_d (sq)	K_d (hq)	(mV)	(mV)
riboflavin	444	374	–	–	–	−231[d]	−167[e]
FMN	445[a]	373[a]	–	–	–	−238[e]	−172[e]
wild-type flavodoxin	460[a]	378[a]	0.24 nM[b]	7.2 pM[c]	0.28 μM[c]	−148	−443
riboflavin complex	460	378	0.51 μM	0.45 μM[c]	15 μM[c]	−228	−257

[a] Swenson and Krey (1994). [b] Curley *et al*. (1991). [c] From the free energy diagram of Dubourdieu *et al*. (1975). [d] Lowe and Clark (1956). [e] Draper and Ingraham (1968).

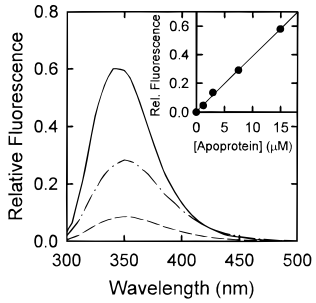

FIGURE 10: Determination of the dissociation constant for the reduced riboflavin complex. The emission spectra of a 15 μM solution of apoflavodoxin in the absence (solid line) and presence of 32 μM (dot-dashed line) and 100 μM (dashed line) reduced riboflavin. Fluorescence quenching is associated with the formation of the apoflavodoxin−riboflavin complex. The inset shows the correlation between the protein fluorescence at 350 nm and apoflavodoxin concentration under these conditions. The excitation wavelength in each case is 290 nm.

riboflavin semiquinone and hydroquinone, respectively. These values are 63000- and 54-fold higher than those of the FMN complex (7.2 pM and 0.28 μM, respectively). The properties of the riboflavin complex and their comparison to those for the recombinant wild-type holoprotein are summarized in Table 1.

The relatively high K_d calculated for the riboflavin hydroquinone complex raised the question as to whether the flavin hydroquinone was dissociating during the redox potential determination, resulting in an error in the midpoint potential for the sq/hq couple of the riboflavin complex. Therefore, the dissociation constant for the hydroquinone form riboflavin complex was also determined directly by fluorimetry under anaerobic conditions. Reduced flavins are believed to be nonfluorescent (Ghisla *et al.*, 1974). Protein fluorescence of the *D. vulgaris* flavodoxin is effectively quenched, and its spectrum could not be measured (D'Anna & Tollin, 1972; Dubourdieu *et al.*, 1975). As observed in the previous reconstitution study, the absorbance changes during the reconstitution of the riboflavin complex are very similar to those of the FMN complex, suggesting that the environment surrounding the isoalloxazine ring in both the riboflavin and FMN complex remains the same. Therefore, the apoflavodoxin fluorescence is assumed to be similarly quenched upon reconstitution with riboflavin. A mixture of apoflavodoxin and riboflavin was reduced anaerobically by light irradiation. The fluorescence of the free apoflavodoxin remaining in solution at equilibrium was monitored by the emission at 350 nm with an excitation wavelength at 290 nm (Figure 10). The apoprotein concentration was determined from the relative fluorescence determined under identical conditions (Figure 10, inset). An average K_d(hq) value of 18 μM was determined from measurements made at total riboflavin concentrations of 100 and 32 μM. The total apoflavodoxin concentration (15 μM) was the same in each case. This value is in good agreement with that (15 μM) calculated from the free energy diagram.

DISCUSSION

The contribution of the negative charge on the 5′-phosphate group of the FMN cofactor to the oxidation−reduction potentials of the *D. vulgaris* flavodoxin was investigated in this study. The phosphate binding site in the flavodoxin is often referred to as being rather unusual because of the absence of basic residues for ion pairing as is generally noted in nucleotide binding sites, a situation even more striking in that the 5′-phosphate is thought to remain dianionic over a broad pH range (Moonen & Müller, 1982; Vervoort *et al.*, 1986a). Instead, X-ray crystallographic (Watenpaugh *et al*., 1973; Watt *et al*., 1991) and two-dimensional NMR studies (Peelen & Vervoort, 1994) of the oxidized flavodoxin holoprotein suggest that the phosphate group may be bound through a network of nine to ten hydrogen bonds with amide nitrogens of the peptide backbone and the hydroxyl oxygen of threonine and serine residues. The conservation of this general binding theme in all other flavodoxin proteins has prompted speculation that the uncompensated charges on the phosphate may have functional significance, perhaps contributing to the very low reduction potential of the sq/hq couple through unfavorable electrostatic interactions with the flavin hydroquinone anion (Moonen *et al.*, 1984).

Histidine mutants of the *D. vulgaris* flavodoxin were designed in this study to probe the intensity of the electrostatic effect of the 5′-phosphate group on the redox properties of the FMN cofactor. The initial goal was to introduce one or more basic amino acid residues at critical positions on the phosphate binding loop without significantly interrupting the hydrogen-bonding network which seems to be important for cofactor binding. Histidine was chosen because the cationic imidazole side chain could be positioned close to and even form direct contacts with the phosphate group. Histidine also has a convenient ionization constant such that its charge can be readily altered over a pH range compatible with the stability of the protein. After several possibilities were screened through molecular modeling and molecular mechanical calculations, two mutant structures were selected, T12H and N14H mutants. Both structures place the basic imidazole side chain adjacent to the phosphate group while potentially maintaining hydrogen-bonding interactions and loop structures similar to those of the wild type. At the outset, it was hoped that two different situations could be studied. The conservative N14H mutation was designed to place the imidazole side chain close to the phosphate but without direct interactions. In the T12H mutant, the His12 side chain could potentially form a strong hydrogen-bonded ion pair with the phosphate group (Figure 2 and Scheme 1). Depending on the relative pK_a values of the two groups

Scheme 1: Potential Hydrogen-Bonded Ion-Pairing Interaction between the Phosphate Group and the His12 Imidazole Side Chain in the T12H Mutant, Including Two Possible Ionization States

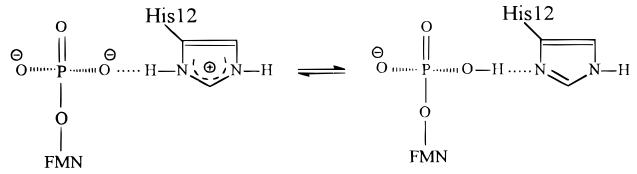

involved, such an interaction could result in the protonation of the phosphate moiety, reducing its negative charge. In this way, the electrostatic effect of the phosphate group on the redox potential could be directly determined. In this situation, the protonation of the phosphate should be indicated by an upfield shift of the ^{31}P NMR resonance (Vervoort *et al.*, 1986a) and perhaps a substantial change in the pK_a value of His12 (Anderson *et al.*, 1991). A second possibility is that hydrogen bonding is not possible due to structural or steric constraints of the imidazole side chain, or the entropic cost of localizing a solvent-exposed imidazole side chain that offsets its interaction energy with the phosphate (Dao-pin *et al.*, 1991). This type of interaction should not alter the ionization state of the 5′-phosphate. However, as for the N14H mutation, there is still the possibility of a general electrostatic interaction between the histidine cation and the phosphate in this situation, more indirectly offsetting its charge through longer range interactions. In this case, the electrostatic effect of the phosphate group could be estimated by the compensating effect of the introduced histidine residue. The strength of the electrostatic interaction between the phosphate group and the histidine residues can be evaluated by the shift in their pK_a values.

The ^{31}P NMR titrations (Figure 5) provided convincing evidence that, although the environment of the 5′-phosphate groups may be perturbed somewhat in both the T12H and N14H mutants, the phosphate group does not appear to change its ionization state over the pH range of 6−8 just as in the wild type. Therefore, the introduction of a neighboring histidine residue has apparently not appreciably altered the apparently unusually low pK_a value of the phosphate (however, see below). The ^{1}H NMR titrations of both histidine mutants (Figures 7 and 8) provided pK_a values for His12 and His14 of 6.71 and 6.93, respectively. The slightly higher pK_a value for His14 could be the consequence of its juxtaposition to Asp129 in the modeled structure. Although both histidine residues display somewhat elevated pK_a values when compared to the average experimental pK_a value of 6.56 for histidine residues in proteins (Markley, 1975), the shifts were much more modest than anticipated for this location. This rather surprising observation plus the absence of a change in the ionization state of the 5′-phosphate seem to exclude the possibility for a direct hydrogen-bonded ion-pairing interaction between the His12 imidazole side chain and the 5′-phosphate group as predicted by the initial model building. Therefore, the electrostatic effect of the phosphate group on the redox potential could not be directly determined in this study from the manipulation of the ionization state of the phosphate group itself.

The ^{1}H NMR experiments, however, do provide some important information about the strength of the electrostatic interaction between the phosphate group and the introduced histidine residues as well as with the charge on the FMN hydroquinone anion. According to Coulomb's Law, the electrostatic interaction energy (ΔG) between the histidine and phosphate groups can be estimated using the formula $\Delta G = 332 z_P z_H / r\epsilon_{eff}$, where z_P and z_H are the charges on the phosphate and histidine, respectively, r is the distance between the two charges in angstroms, and ϵ_{eff} is the effective dielectric constant (Russell *et al.*, 1987). Alternatively, the shift in pK_a that might result from this electrostatic interaction can be calculated by the equation, $\Delta pK_a = 244 z_P z_H / r\epsilon_{eff}$. As always, the determination of ϵ_{eff} is complicated by the discontinuity and nonhomogeneity inherent in protein systems. However, on the basis of pK_a shifts, a good correlation between experimental and theoretical results has been established for long range electrostatic interactions using the above relationships [for example, see Russell *et al.* (1987)]. Molecular-modeling studies suggest that both His12 and His14 are on the surface and solvent accessible, placing the imidazole at the interface between the relatively high dielectric environment of the solvent and the heterogeneous but lower dielectric environment provided by the protein. On the basis of analogy with the Russell *et al.* (1987) study involving surface residues, a value of 75 for ϵ_{eff} seems appropriate under the solvent conditions and ionic strength used in the NMR study (see also below). For an average charge separation of 4−5 Å based on the molecular-modeling studies, and charges of +1 and −2 on the histidine and 5′-phosphate, respectively, a pK_a shift of 1.3−1.6 for the introduced histidine residue was anticipated under these conditions. Even if the histidine side chain is extended as far as possible from the phosphate while maintaining similar positioning of the main chain as in the wild-type structure (∼9 Å), the calculated pK_a shift (∼0.7) is considerably larger than observed. Using the observed ΔpK_a values and r values ranging from 4 to 9 Å, unrealistically high values for the effective dielectric constants are calculated (>200). These results seem to suggest that the effective charge on the 5′-phosphate group might actually be less than the formal dianionic charge set for this group. On the basis of the observed pK_a shifts of 0.15−0.37 relative to an average pK_a for histidine, an ϵ_{eff} of 75, and distances ranging from 4 to 9 Å, the charge on the phosphate can be calculated to fall between −0.2 and −1. How can this be? Two explanations can be offered. Although there are no basic residues adjacent to the 5′-phosphate in the wild-type holoprotein with which to offset its charge, the phosphate group is hydrogen-bonded to an extensive network of dipolar NH and OH groups contributed by the backbone and side chains (Figure 1) (Watt *et al.*, 1991). Together, these dipoles may partially offset and/or shield the negative charges of the phosphate, resulting in a lower effective charge as the results of this study suggest. Alternatively, these results may indicate that the ^{31}P NMR data are not accurately reflecting the actual ionization state of the 5′-phosphate group. Gorenstein (1981) suggests that the chemical shift of the phosphate group is very sensitive to the geometry of the phosphate−oxygen bonds in phosphate mono-, di-, and triesters. In fact, the sensitivity of the ^{31}P chemical shift to changes in the ionization state of acyclic phosphate monoesters has been attributed not so much to the deshielding effects of charge itself but to alterations in the O−P−O bond angle induced by the change in ionization state (Gorenstein, 1981). The extensive hydrogen-bonding network between the protein and the 5′-phosphate may significantly restrict its geometry relative to that in solution. This situation may in fact be more

influential in promoting the substantial downfield shift of the phosphate resonance than the actual ionization state itself. This raises the possibility that the 5′-phosphate may not actually exist as the dianionic species as previously proposed which would be more consistent with our analysis of the effective charge on the 5′-phosphate based on the histidine pK_a values.

Even if one accepts the formal charge of −2 on the phosphate, the results of this study provide evidence that the electrostatic effect of this charge on $E_{sq/hq}$ should be rather small. This conclusion is based on the electrostatic effects of the charge of the histidine residue in both mutants on the redox potential for the sq/hq couple as evaluated by its pH dependency (Figure 4). The maximum reduction potential shift relative to that of the wild-type holoprotein obtained at low pH values was *ca.* 28 mV for the T12H mutants, with about 18 mV attributed to the ionization of His12, and *ca.* 15 mV for the N14H mutant. These values were within the range of the typical redox potential shift when an acidic residue within 13 Å of the FMN N1 was neutralized, which is 12−18 mV (Zhou & Swenson, 1995). In a separate study, the general electrostatic effect in the vicinity of the flavin was explored by the Tyr100 to His mutation also in the *D. vulgaris* flavodoxin (Helms, 1992; Helms *et al.*, manuscript in preparation). The redox potential for the sq/hq couple in this mutant was also shifted about 18 mV during the ionization of His100. This histidine residue, which is located in a different region of the FMN binding site some distance from the 5′-phosphate group, is about 10−11 Å from the FMN N1, as are His12 (10−12 Å) and His14 (10−11 Å). Thus, the pH-dependent shifts in $E_{sq/nq}$ for these histidine mutants are all consistent with our earlier conclusions that the reduction potential for the sq/hq couple is sensitive to the general electrostatic environment provided by charged groups surrounding the isoalloxazine ring (Zhou & Swenson, 1995). The introduction of an additional histidine residue within an average distance of 11 Å from N1 of the flavin decreases the unfavorable electronegative environment by one formal charge when fully protonated. These results seem to be consistent with theoretical values for the electrostatic interaction predicted from Coulomb's Law. Again, assuming an effective dielectric constant of 75 under these solvent conditions, net charges of +1 and −1 on the histidine and flavin hydroquinone, respectively, and an average charge separation of 11 Å, a ΔG value of 0.40 kcal/mol is calculated. This value is very similar to the free energy change associated with the observed shifts in the reduction potentials for not only the histidine mutants but also those associated with the neutralization of the surrounding acidic residues (Zhou & Swenson, 1995). These electrostatic energies are also in agreement with the experimental and theoretical values obtained by Loewenthal *et al.* (1993) involving long range surface charge−charge interactions in barnase and subtilisin in which interaction energies of 0.3−0.5 kcal/mol between single charges separated by less than 12 Å at low ionic strengths were observed. Therefore, the preponderance of the evidence provided by these studies suggests that within 13.0 Å of the FMN N1 the average electrostatic effect of a single charge (including the acidic residues, the histidines, and possibly the 5′-phosphate group) on the redox potential is about 15 mV. Thus, even if the full effect of the dianionic charge is felt by the flavin hydroquinone anion, the 5′-phosphate group on the FMN cofactor would at the most contribute a 30 mV shift in reduction potential. This estimation of the phosphate electrostatics is also compatible with a study in which the *D. vulgaris* and *M. elsdenii* apoflavodoxins were reconstituted with riboflavin 3′,5′-bisphosphate, an analog containing the additional anionic phosphate moiety (Vervoort *et al.*, 1986b). In this case, the redox potential for the sq/hq couple in the flavodoxin complex was shifted to be about 20 mV more negative than that of the native flavodoxin. In the final analysis, then, it can be concluded that the effective charge on the 5′-phosphate may be substantially less than expected on the basis of its reported formal charge and is, therefore, not likely to be a significant factor in the modulation of the reduction potentials of the bound flavin cofactor in this flavodoxin, particularly for the sq/hq couple.

These conclusions appear to be contrary to theoretical calculations (Moonen *et al.*, 1984) and to the reconstitution of apoflavodoxin with riboflavin which effectively "removes" any electrostatic effects of the 5′-phosphate group of the cofactor (Curley *et al.*, 1991). Both results suggest that the 5′-phosphate could decrease the reduction potential of the sq/hq couple by as much as 180 mV. The substantial disparity between these results and those obtained for the histidine mutants in this study prompted the re-evaluation of the redox properties of our recombinant apoprotein preparation reconstituted with riboflavin. Values for $E_{ox/sq}$ and $E_{sq/hq}$ of −228 and −257 mV were determined at pH 7.0, respectively. When differences in pH are considered, these results correspond quite well to values of −193 and −262 mV at pH 6.50 that are reported by Curley *et al.* (1991b).

The absence of the phosphate group in the riboflavin complex undoubtedly disrupts the hydrogen-bonding network between the cofactor and the protein in this region. This is reflected in large increases in the dissociation constants of the riboflavin complexes. The K_d values for the oxidized, semiquinone, and fully reduced states are 0.51, 0.45, and 15 μM, respectively, with the latter two constants being derived indirectly from the reduction potentials compared to that of unbound FMN. However, a K_d value of 18 μM for the hydroquinone state, which was determined more directly by fluorescence quenching in this study, is in good agreement with the calculated value and provides independent confirmation of the much less negative midpoint potential for the sq/hq couple of the riboflavin complex. These K_d values are 2100-, 63000-, and 54-fold higher than those of the wild-type flavodoxin, equivalent to the losses in binding energy of 4.5, 8.9, and 2.4 kcal/mol for the oxidized, semiquinone, and hydroquinone states, respectively. Therefore, the semiquinone state of the riboflavin complex is more highly destabilized relative to the other oxidation states. Because the semiquinone is a common intermediate, both redox couples are affected such that $E_{ox/sq}$ becomes more negative and $E_{sq/hq}$ is substantially less negative than the FMN complex. It was demonstrated previously that there was no obvious correlation between the $E_{ox/sq}$ value and the electrostatic environment of the cofactor (Zhou & Swenson, 1995). It is unlikely, then, that the decrease of 79 mV for the midpoint potential of the ox/sq couple for the riboflavin complex relative to that of the normal holoprotein is the consequence of the loss of any electrostatic effects of the 5′-phosphate**.** Similarly, the results of this study provide evidence that the electrostatic contribution of the phosphate group to the reduction potential of the sq/hq couple is relatively small, perhaps contributing no more than 30 mV

to the shift in potential of the cofactor or equivalent to the sum of two surface acidic amino acid residues (Zhou & Swenson, 1995). This estimation implies that only a small portion of the redox potential increase of 186 mV for the sq/hq couple in the riboflavin complex can be attributed to the loss of any electrostatic effects of the phosphate group. Most of the change must be due to a disproportionate loss in binding energy in the semiquinone state. The structure of the phosphate binding loop does not appear to change upon change in the oxidation state of the flavin (Watt *et al.*, 1991); therefore, it is difficult to rationalize the differential effect of the absence of the phosphate group in the riboflavin complex. It is possible that the conformation of the phosphate binding loop is different in the riboflavin complex, and this structural difference is translated to other regions of the cofactor binding site which interact more directly with the isoalloxazine ring. Until the structure of the riboflavin complex is elucidated, the molecular basis of this effect may remain poorly understood.

ACKNOWLEDGMENT

We thank Dr. Charles E. Cottrell of The Ohio State University Campus Chemical Instrument Center for his assistance in obtaining the FT-NMR spectra.

REFERENCES

Anderson, D. E., Becktel, W., & Dahlquist, F. W. (1990) *Biochemistry 29*, 2403−2408.
Bird, C. L., & Kuhn, A. T. (1981) *Chem. Soc. Rev. 10*, 49−82.
Cammack, R., Rao, K., Hall, D., Moura, J., Xavier, A., Bruschi, M., LeGall, J., Deville, A., & Gayda, J. (1997) *Biochim. Biophys. Acta 490*, 311−321.
Clark, W. M. (1972) in *Oxidation-Reduction Potentials of Organic Systems*, pp 107−148, 412−417, Robert E. Krieger Publishing Co., New York.
Curley, G. P., Carr, M. C., Mayhew, S. G., & Voordouw, G. (1991) *Eur. J. Biochem. 202*, 1091−1100.
D'Anna, J. A., Jr., & Tollin, G. (1972) *Biochemistry 11*, 1073−1080.
Dao-pin, S., Sauer, U., Nicholson, H., & Matthews, B. W. (1991) *Biochemistry 30*, 7142−7153.
Draper, R. D., & Ingraham, L. L. (1968) *Arch. Biochem. Biophys. 125*, 802−808.
Dubourdieu, M., LeGall, J., & Favaudon, V. (1975) *Biochim. Biophys. Acta 376*, 519−532.
Dutton, P., & Baltscheffsky, M. (1972) *Biochim. Biophys. Acta 267*, 172−178.
Elwell, M. L., & Schellman, J. A. (1977) *Biochim. Biophys. Acta 494*, 367−383.
Ghisla, S., Massey, V., Lhoste, J.-M., & Mayhew, S. G. (1974) *Biochemistry 13*, 589−597.
Gorenstein, D. G. (1981) *Annu. Rev. Biophys. Bioeng. 10*, 355−386.
Helms, L. R. (1992) Ph.D. Thesis, The Ohio State University, Columbus, OH.
Homer, R. F., Mees, G. C., & Tomlinson, T. E. (1960) *J. Sci. Food Agric. 11*, 309−315.
Kazarinova, N. F., Solomko, K. A., & Kotelenets, M. N. (1967) *Chem. Abstr. 67*, 2975d.
Krey, G. D., Vanin, E. F., & Swenson, R. P. (1988) *J. Biol. Chem. 244*, 15436−15443.
Kunkel, T. A. (1985) *Proc. Natl. Acad. Sci. U.S.A. 82*, 488−492.
Loewenthal, R., Sancho, J., Reinikainen, T., & Fersht, A. R. (1993) *J. Mol. Biol. 232*, 574−583.
Lowe, H. J., & Clark, W. M. (1956) *J. Biol. Chem. 221*, 983−992.
Ludwig, M. L., & Luschinsky, C. L. (1992) in *Chemistry and Biochemistry of Flavoenzymes* (Müller, F., Ed.) Vol. III, pp 427−466, CRC Press, Boca Raton, FL.
Ludwig, M. L., Schopfer, L. M., Metzger, A. L., Pattridge, K. A., & Massey, V. (1990) *Biochemistry 29*, 10364−10375.
Markley, J. L. (1973) *Biochemistry 12*, 2245−2249.
Markley, J. L. (1975) *Acc. Chem. Res. 8*, 70−80.
Mayhew, S. G., & Ludwig, M. L. (1975) in *The Enzymes* (Boyer, P. D., Ed.) 3rd ed., Vol. 12, pp 57−118, Academic Press, New York.
Mayhew, S. G., & Tollin, G. (1992) in *Chemistry and Biochemistry of Flavoenzymes* (Müller, F., Ed.) Vol. III, pp 389−426, CRC Press, Boca Raton, FL.
Moonen, C. T. W., & Müller, F. (1982) *Biochemistry 21*, 408−414.
Moonen, C. T. W., Vervoort, J., & Müller, F. (1984) in *Flavins and Flavoproteins* (Bray, R. C., Engel, P. C., & Mayhew, S. G., Eds.) pp 493−496, Walter de Gruyter & Co., Berlin.
Müller, F. (1992) in *Chemistry and Biochemistry of Flavoenzymes* (Müller, F., Ed.) Vol. I, p 45, CRC Press, Boca Raton, FL.
Peelen, S., & Vervoort, J. (1994) *Arch. Biochem. Biophys. 314*, 291−300.
Russell, A. J., Thomas, P. G., & Fersht, A. R. (1987) *J. Mol. Biol. 193*, 803−813.
Sanger, F., Nicklen, S., & Coulson, A. R. (1977) *Proc. Natl. Acad. Sci. U.S.A. 74*, 5463−5467.
Swenson, R. P., & Krey, G. D. (1994) *Biochemistry 33*, 8505−8514.
Vervoort, J., Müller, F., Mayhew, S. G., van den Berg, W. A. M., Moonen, C. T. W., & Bacher, A. (1986a) *Biochemistry 25*, 6789−6799.
Vervoort, J., van Berkel, W. J. H., Mayhew, S. G., Müller, F., Bacher, A., Nielsen, P., & LeGall, J. (1986b) *Eur. J. Biochem. 161*, 749−756.
Wassink, J. H., & Mayhew, S. G. (1975) *Anal. Biochem. 68*, 609−616.
Watenpaugh, K. D., Sieker, L. C., & Jensen, L. H. (1973) *Proc. Natl. Acad. Sci. U.S.A. 70*, 3857−3860.
Watenpaugh, K. D., Sieker, L. C., & Jensen, L. H. (1976) in *Flavin and Flavoproteins* (Singer, T. P., Ed.) pp 405−410, Elsevier, Amsterdam.
Watt, W., Tulinsky, A., Swenson, R. P., & Watenpauph, K. D. (1991) *J. Mol. Biol. 218*, 195−208.
Weiner, S. J., Kollman, P. A., Nguyen, D. T., & Case, D. A. (1986) *J. Comput. Chem. 7*, 230−252.
Zhou, Z., & Swenson, R. P. (1995) *Biochemistry 34*, 3183−3192.

BI9610865